

## Determinants of the Hepatitis C Virus Nonstructural Protein 2 Protease Domain Required for Production of Infectious Virus<sup>∇</sup>

Thomas G. Dentzer,<sup>1,2</sup> Ivo C. Lorenz,<sup>1†</sup> Matthew J. Evans,<sup>1‡</sup> and Charles M. Rice<sup>1\*</sup>

Center for the Study of Hepatitis C, Laboratory of Virology and Infectious Disease, The Rockefeller University, 1230 York Avenue, New York, New York 10065,<sup>1</sup> and Laboratoire de Rétrovirologie, Centre de Recherche Public-Santé, 84 rue Val Fleuri, Luxembourg L-1526, Luxembourg<sup>2</sup>

Received 9 June 2009/Accepted 28 September 2009

**The hepatitis C virus (HCV) nonstructural protein 2 (NS2) is a dimeric multifunctional hydrophobic protein with an essential but poorly understood role in infectious virus production. We investigated the determinants of NS2 function in the HCV life cycle. On the basis of the crystal structure of the postcleavage form of the NS2 protease domain, we mutated conserved features and analyzed the effects of these changes on polyprotein processing, replication, and infectious virus production. We found that mutations around the protease active site inhibit viral RNA replication, likely by preventing NS2-3 cleavage. In contrast, alterations at the dimer interface or in the C-terminal region did not affect replication, NS2 stability, or NS2 protease activity but decreased infectious virus production. A comprehensive deletion and mutagenesis analysis of the C-terminal end of NS2 revealed the importance of its C-terminal leucine residue in infectious particle production. The crystal structure of the NS2 protease domain shows that this C-terminal leucine is locked in the active site, and mutation or deletion of this residue could therefore alter the conformation of NS2 and disrupt potential protein-protein interactions important for infectious particle production. These studies begin to dissect the residues of NS2 involved in its multiple essential roles in the HCV life cycle and suggest NS2 as a viable target for HCV-specific inhibitors.**

An estimated 130 million people are infected with hepatitis C virus (HCV), the etiologic agent of non-A, non-B viral hepatitis. Transmission of the virus occurs primarily through blood or blood products. Acute infections are frequently asymptomatic, and 70 to 80% of the infected individuals are unable to eliminate the virus. Of the patients with HCV-induced chronic hepatitis, 15 to 30% progress to cirrhosis within years to decades after infection, and 3 to 4% of patients develop hepatocellular carcinoma (17). HCV infection is a leading cause of cirrhosis, end-stage liver disease, and liver transplantation in Europe and the United States (7), and reinfection after liver transplantation occurs almost universally. There is no vaccine available, and current HCV therapy of pegylated alpha interferon in combination with ribavirin leads to a sustained response in only about 50% of genotype 1-infected patients.

The positive-stranded RNA genome of HCV is about 9.6 kb in length and encodes a single open reading frame flanked by 5' and 3' nontranslated regions (5' and 3' NTRs). The translation product of the viral genome is a large polyprotein containing the structural proteins (core, envelope proteins E1 and E2) in the N-terminal region and the nonstructural proteins (p7, nonstructural protein 2 [NS2], NS3, NS4A, NS4B, NS5A, and NS5B) in the C-terminal region. The individual proteins

are processed from the polyprotein by various proteases. The host cellular signal peptidase cleaves between core/E1, E1/E2, E2/p7, and p7/NS2, and signal peptide peptidase releases core from the E1 signal peptide. Two viral proteases, the NS2-3 protease and the NS3-4A protease, cleave the remainder of the viral polyprotein in the nonstructural region (22, 27). The structural proteins package the genome into infectious particles and mediate virus entry into a naïve host cell; the nonstructural proteins NS3 through NS5B form the RNA replication complex. p7 and NS2 are not thought to be incorporated into the virion but are essential for the assembly of infectious particles (14, 36); however, their mechanisms of action are not understood.

NS2 (molecular mass of 23 kDa) is a hydrophobic protein containing several transmembrane segments in the N-terminal region (5, 9, 32, 39). The C-terminal half of NS2 and the N-terminal third of NS3 form the NS2-3 protease (10, 11, 26, 37). NS2 is not required for the replication of subgenomic replicons, which span NS3 to NS5B (20). However, cleavage at the NS2/3 junction is necessary for replication in chimpanzees (16), the full-length replicon (38), and in the infectious tissue culture system (HCVcc) (14). Although cleavage can occur in vitro in the absence of microsomal membranes, synthesis of the polyprotein precursor in the presence of membranes greatly increases processing at the NS2/3 site (32). In vitro studies indicate that purified NS2-3 protease is active in the absence of cellular cofactors (11, 37). In addition to its role as a protease, NS2 has been shown to be required for assembly of infectious intracellular virus (14). The N-terminal helix of NS2 was first implicated in infectivity by the observation that an intergenotypic breakpoint following this transmembrane segment resulted in higher titers of infectious virus (28). Structural and

\* Corresponding author. Mailing address: Laboratory of Virology and Infectious Disease, Center for the Study of Hepatitis C, The Rockefeller University, 1230 York Ave., New York, NY 10065. Phone: (212) 327-7046. Fax: (212) 327-7048. E-mail: ricec@rockefeller.edu.

† Present address: International AIDS Vaccine Initiative, AIDS Vaccine Design & Development Laboratory, Brooklyn, NY 11220.

‡ Present address: Department of Microbiology, Mount Sinai School of Medicine, New York, NY 10029.

<sup>∇</sup> Published ahead of print on 7 October 2009.

functional characterization of the NS2 transmembrane region has shown that this domain is essential for infectious virus production (13). In particular, a central glycine residue in the first NS2 helix plays a critical role in HCV infectious virus assembly (13). The NS2 protease domain, but not its catalytic activity, is also essential for infectious virus assembly, whereas the unprocessed NS2-3 precursor is not required (13, 14).

The crystal structure of the postcleavage NS2 protease domain (NS2<sup>Pro</sup>, residues 94 to 217), revealed a dimeric cysteine protease containing two composite active sites (Fig. 2C; [21]). Two antiparallel  $\alpha$ -helices make up the N-terminal subdomain, followed by an extended crossover region, which positions the  $\beta$ -sheet-rich C-terminal subdomain near the N-terminal region of the partner monomer. Two of the conserved residues of the catalytic triad (His 143, Glu 163) are located in the loop region after the second N-terminal helix of one monomer, while the third catalytic residue, Cys 184, is located in the C-terminal subdomain of the other monomer. Creation of this unusual pair of composite active sites through NS2 dimerization has been shown to be essential for autoproteolytic cleavage (21). The structure of NS2<sup>Pro</sup> further demonstrated that the C-terminal residue of NS2 remains bound in the active site after cleavage, suggesting a possible mechanism for restriction of this enzyme to a single proteolytic event (21). Here we have used the crystal structure of NS2<sup>Pro</sup>, along with sequence alignments, to target conserved residues in each of the NS2<sup>Pro</sup> structural regions. Our mutational analysis revealed that the residues in the dimer crossover region and the C-terminal subdomain are important for infectious virus production. In contrast, the majority of amino acids in the active site pocket were not required for infectivity. Interestingly, we observed that the extreme C-terminal leucine of NS2 is absolutely essential for generation of infectious virus, as mutations, deletions, and extensions into NS3 are very poorly tolerated. This analysis begins to dissect the determinants of the multiple functions of this important protease in the HCV life cycle.

## MATERIALS AND METHODS

**Plasmid constructs.** Mono- and bicistronic (see Fig. 1A) genomes were generated by standard molecular biology techniques and verified by restriction enzyme digestion and sequencing of PCR-amplified segments. Descriptions of the cloning strategies are provided below, and plasmid and primer sequences are available upon request.

(i) **J6/H77NS2/JFH and mutant derivatives.** J6/H77NS2/JFH constructs contain genotype 2a (J6) from core to p7, genotype 1a (strain H77) NS2 and genotype 2a (JFH) NS3 to NS5B. To create this construct, the J6/JFH plasmid (18) was used as a template to PCR amplify the J6/JFH E2 3' end through the p7 sequence with forward oligonucleotide RU-O-5739 (5'-CCGCTTGTCGA CTGGTC) and reverse oligonucleotide RU-O-5855 (5'-CTCCGTGTC-CAACGCGTAAGCCTGTTGGGGC). The H77 NS2 through half of JFH-1 NS3 region was PCR amplified from H77/JFH (18) with the forward oligonucleotide RU-O-5854 (5'-CAGGCTTACGCGTTGGACACGGAGGTGGCC) and reverse oligonucleotide RU-O-5721 (5'-GCTACCGAGGGGTTAAGCA CT). Since these PCR products overlap at the p7/NS2 junction, they were used as template in a second round of PCR with the outside oligonucleotides RU-O-5855 and RU-O-5721 to generate a PCR product encoding the J6 E2 C-terminal region through p7, the H77 NS2, and JFH-1 NS3 N-terminal region. This product was digested with restriction endonucleases BsaBI and AvrII and ligated into the BsaBI/AvrII-digested J6/JFH plasmid to create the final J6/H77NS2/JFH plasmid. An adaptive change at G1145A (chimeric genome numbering) encoding substitution A269T (chimeric polyprotein numbering) was found to increase infectious virus titers of J6/H77NS2/JFH, and was included in all J6/H77NS2/

JFH-based genomes constructed. Mutant derivatives of J6/H77NS2/JFH were created by site-directed mutagenesis using the AfeI/BbvCI restriction sites.

(ii) **J6/H77NS2/JFH(NS2-IRES-NS3) and mutant derivatives.** J6/H77NS2/JFH(NS2-IRES-NS3) encodes a stop codon after NS2, an encephalomyocarditis virus (EMCV) internal ribosome entry site (IRES), a start codon, and the remainder of the JFH-1 polyprotein starting with NS3. Mutant derivatives of J6/H77NS2/JFH(NS2-IRES-NS3) were created by site-directed mutagenesis using the PmeI/MluI restriction sites.

(iii) **J6/H77NS2/JFH(NS2-IRES-nsGluc2AUbi) and mutant derivatives.** J6/H77NS2/JFH(NS2-IRES-nsGluc2AUbi) is similar to J6/H77NS2/JFH(NS2-IRES-NS3) but encodes a *Gaussia* luciferase gene followed by the foot and mouth disease virus 2A peptide and a ubiquitin monomer (nsGluc2AUbi cassette) between the EMCV IRES and NS3 (14). The N-terminal signal sequence of *Gaussia* luciferase has been deleted so that the reporter is not secreted. Mutant derivatives of J6/H77NS2/JFH(NS2-IRES-nsGluc2AUbi) were created by site-directed mutagenesis using the PmeI/MluI restriction sites. NS2 extensions into NS3 were subcloned using BbvCI/SpeI/KpnI restriction sites.

**Cell culture.** Huh-7.5 cells were cultured in Dulbecco's modified Eagle medium (Invitrogen) supplemented with 0.1 mM nonessential amino acids and 10% fetal bovine serum (complete medium). Cells were grown at 37°C in 5% CO<sub>2</sub>.

**RNA transcription.** In vitro transcripts were generated as previously described (18). Briefly, plasmid DNA was linearized by XbaI and purified by using a Minelute column (Qiagen, Valencia, CA). RNA was transcribed from 1  $\mu$ g of purified template by using the T7 Megascript kit (Ambion, Austin, TX) or the T7 RNA polymerase kit (Promega, Madison, WI). Reaction mixtures were incubated at 37°C for 3 h, followed by a 15-min digestion with 3 U of DNase I (Ambion). RNA was purified by using an RNeasy kit (Qiagen) with an additional on-column DNase treatment. RNA was quantified by absorbance at 260 nm and diluted to 0.5  $\mu$ g/ $\mu$ l. Prior to storage at -80°C, RNA integrity was determined by agarose gel electrophoresis and visualization by ethidium bromide staining.

**RNA electroporation.** Huh-7.5 cells were electroporated with RNA as previously described (18). Briefly, Huh-7.5 cells were treated with trypsin, washed twice with ice-cold RNase-free AccuGene phosphate-buffered saline (PBS) (Bio-Whittaker, Rockland, ME), and resuspended at  $1.75 \times 10^7$  cells/ml in PBS. Then, 2  $\mu$ g of each RNA was combined with 0.4 ml of cell suspension and immediately pulsed using a BTX ElectroSquare Porator ECM 830 (820 V, 99  $\mu$ s, five pulses). Electroporated cells were incubated at room temperature for 10 min prior to resuspension in 15 ml or 30 ml complete medium for nonreporter and reporter constructs, respectively. Resuspended cells were plated into 24-well, 6-well, and P100 tissue culture dishes.

**Assays for RNA replication.** At 4 or 8, 24, 48, and 72 h postelectroporation, cells in 24-well plates were washed with Dulbecco PBS and lysed by the addition of *Renilla* lysis buffer (Promega, Madison, WI) or RLT buffer (Qiagen) containing 1%  $\beta$ -mercaptoethanol for assay of replication by luciferase activity or quantitative reverse transcription-PCR (qRT-PCR), respectively. For luciferase assays, the lysates were thawed prior to the addition of *Renilla* substrate (Promega) according to the manufacturer's instructions. The luciferase activity was measured by using a Berthold Centro LB 960 96-well luminometer. For qRT-PCR analysis, prior to storage at -80°C, the lysates were homogenized by centrifugation through a QiaShredder column (Qiagen) for 2 min at  $14,000 \times g$ . Total RNA was isolated by RNeasy kit (Qiagen) and quantified by determining the absorbance at 260 nm. A total of 50 ng of total cellular RNA was used per reaction mixture. qRT-PCRs were performed on a LightCycler 480 (Roche, Basel, Switzerland) using the LightCycler amplification kit (Roche) with primers directed against the viral 3' NTR. We assembled 20- $\mu$ l reaction mixtures according to the manufacturer's instructions as previously described (14).

**Assays for infectious virus production.** At 4 or 8, 24, 48, and 72 h postelectroporation, the cell culture medium was harvested and replaced with fresh complete medium. Harvested cell culture supernatants were clarified by using a 0.45- $\mu$ m-pore-size filter and stored in aliquots at -80°C. For detection of infectious virus production by qRT-PCR or luciferase assay, naïve cells were infected with clarified cell culture supernatants and incubated for 72 h prior to analysis. Determination of infectious virus production by limiting dilution assay was performed as described previously (14, 18). Briefly, clarified cell culture supernatants were serially diluted and used to infect approximately  $3 \times 10^3$  cells plated in 96-well dishes. At 3 days postinfection, cells were washed with Dulbecco PBS, fixed with ice-cold methanol, and stained for the presence of NS5A expression as described previously. The 50% tissue culture infectious dose (TCID<sub>50</sub>) was calculated using the Reed and Muench method (18).

**Anti-NS2 Mab (6H6).** The immunogen was a recombinant NS2 protease domain of strain H77 (residues 94 to 217 with an amino-terminal hexahistidine tag) expressed in *Escherichia coli* and purified by fast protein liquid chromatog-

raphy under denaturing conditions (6 M guanidinium hydrochloride) or in the presence of detergent (21). BALB/c mice were immunized three times intraperitoneally with 50  $\mu$ g NS2 purified under denaturing conditions, followed by a final boost with 50  $\mu$ g NS2 purified in the presence of detergent. The preimmune and test bleeds were assayed for the presence of NS2-specific polyclonal antibodies by a standard enzyme-linked immunosorbent assay, as well as by Western blotting. Screening of hybridoma supernatants produced 6H6, an isotype immunoglobulin G1 monoclonal antibody (MAb).

**SDS-PAGE and immunoblotting.** Cells were lysed at 72 h postelectroporation with RLT buffer (Qiagen) containing 1%  $\beta$ -mercaptoethanol and homogenized by centrifugation through a QiaShredder column (Qiagen) for 2 min at 14,000  $\times$  g. The lysates were separated by sodium dodecyl sulfate-polyacrylamide gel electrophoresis (SDS-PAGE). After transfer to nitrocellulose membrane, the blots were blocked for 1 h with 5% milk-PBS-T (PBS plus 0.1% Tween). For NS2 detection, MAb 6H6 (1.0 mg/ml) was diluted 1:1,000 in PBS-T. For NS5A detection, MAb 9E10 (18) was diluted 1:1,000 in PBS-T. For  $\beta$ -actin detection, mouse anti- $\beta$ -actin MAb (Sigma, St. Louis, MO) was diluted 1:20,000 in PBS-T. After 1-h incubation at room temperature and extensive washing with PBS-T, horseradish peroxidase-conjugated rabbit anti-mouse immunoglobulin secondary antibody (Pierce, Rockford, IL) was added at 1:10,000 dilution in 5% milk-PBS-T for 45 min at room temperature. After additional washing, blots were developed with SuperSignal West Pico chemiluminescent substrate (Pierce).

## RESULTS

**Creation and characterization of triple chimeric HCV genomes.** The crystal structure of NS2<sup>PRO</sup> was solved using the H77 genotype 1a protein (21). In order to facilitate a structure-based mutational analysis of NS2, we created J6/JFH genomes encoding the H77 NS2 sequence. Three different full-length HCV genome constructs were used (Fig. 1A). J6/H77NS2/JFH is a monocistronic genome encoding J6 core through p7, H77 NS2, and JFH-1 NS3 through NS5B; the 5' and 3' NTRs of all the genomes are derived from JFH-1. J6/H77NS2/JFH replicated with kinetics similar to those of J6/JFH but released approximately 50-fold-less infectious virus (data not shown). By passaging transfected cells, we selected a single nucleotide change, G1145A (chimeric genome nucleotide numbering) encoding an A269T mutation in the J6 E1 protein. This substitution enhanced infectious particle production (data not shown) and was included in all genomes constructed. To study the functions of NS2 in infectious virus production independent of its autoproteolytic cleavage requirements, we created bicistronic genomes. J6/H77NS2/JFH(NS2-IRES-NS3) is identical to J6/H77NS2/JFH but with the addition of a stop codon after H77 NS2 and an encephalomyocarditis virus internal ribosome entry site upstream of NS3. This genome allows expression of the viral replicase independently of NS2-3 cleavage, and thus uncouples processing from replication and virus production. J6/H77NS2/JFH(NS2-IRES-nsGluc2AUbi) is identical to J6/H77NS2/JFH(NS2-IRES-NS3), but it encodes the reporter gene *Gaussia* luciferase immediately downstream of the EMCV IRES. Cleavage of the reporter protein from the viral polyprotein is mediated by the foot-and-mouth disease virus 2A peptide and cleavage after the C terminus of the ubiquitin monomer by host ubiquitin carboxy-terminal hydrolase (31). This generates nonsecreted *Gaussia* luciferase (ns-Gluc) and the proper N terminus of NS3. The triple chimeric genomes were tested for replication and infectious virus production at various times postelectroporation of Huh-7.5 cells with in vitro-transcribed RNA; 72-h time points are shown (Fig. 1). All chimeric genomes were viable, although RNA replication levels and infectious particle production were somewhat reduced compared to the parental J6/JFH. As ex-

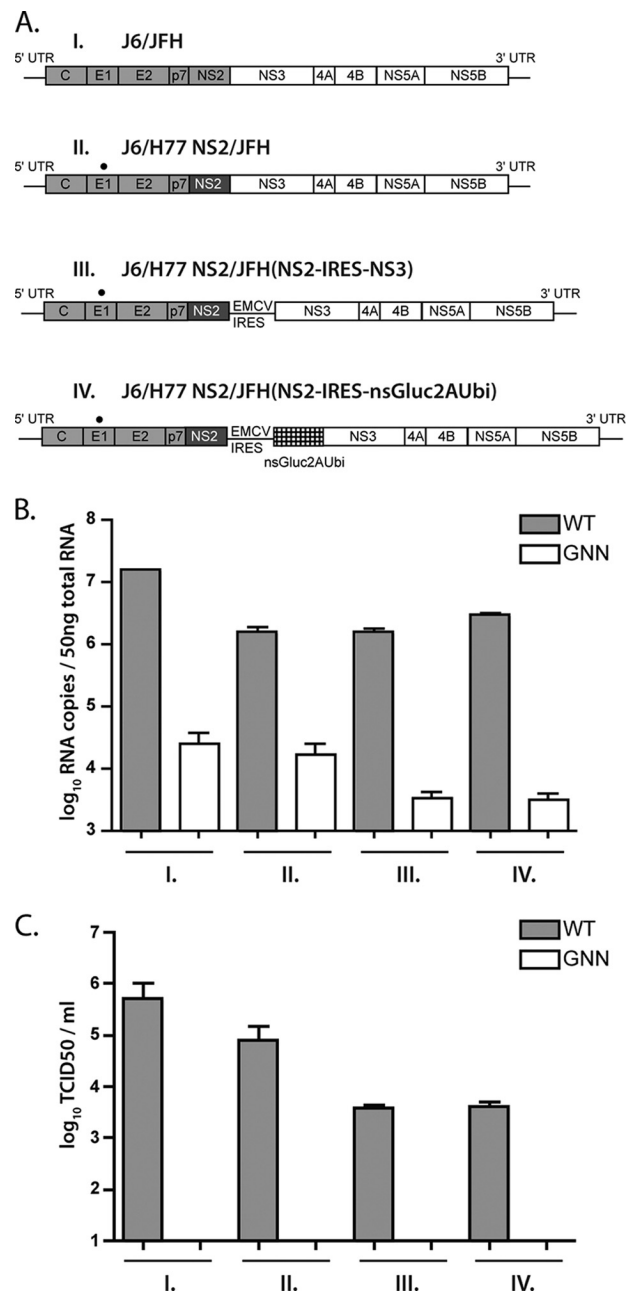


FIG. 1. HCV genomes used in this study. (A) Schematic representation of HCV genomes. (I) J6/JFH with J6 C-NS2 shown in gray and JFH NS3-NS5B in white. (II) J6/H77NS2/JFH with J6 (gray), H77 NS2 (dark gray), and JFH (white) with adaptive mutation in E1 (black dot). (III) Bicistronic construct similar to that shown for construct II but with an EMCV IRES between NS2 and NS3. (IV) Bicistronic reporter construct similar to construct III with EMCV IRES, plus nonsecreted *Gaussia* luciferase, foot and mouth disease virus 2A and ubiquitin cleavage sites (nsGluc2AUbi) between NS2 and NS3 (checked box). 5' UTR and 3' UTR, 5' untranslated region and 3' untranslated region, respectively. (B) RNA replication of J6/JFH and J6/H77/JFH genomes measured by quantitative RT-PCR at 72 h postelectroporation. HCV RNA copies normalized to 50 ng of total RNA. (C) Infectious virus production of bicistronic constructs at 72 h postelectroporation, as measured by limiting dilution assay (TCID<sub>50</sub>). WT, wild type of each genome indicated; GNN, corresponding polymerase-defective control. The means plus standard errors of the means (error bars) of three independent experiments with two different RNA preparations are shown.

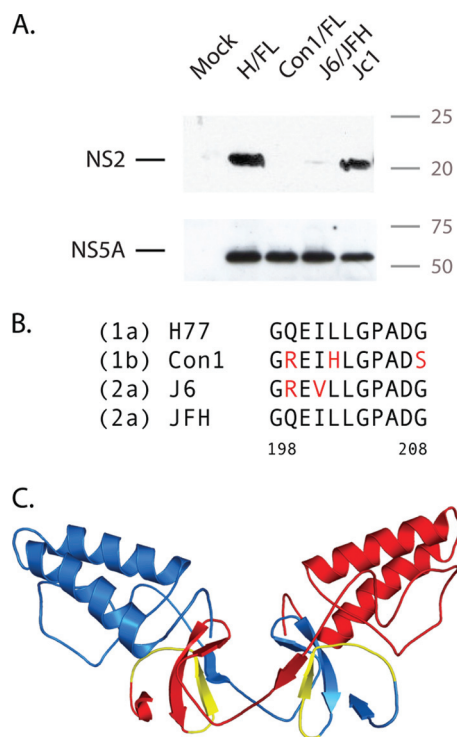


FIG. 2. Characterization of anti-NS2 antibody (6H6). (A) Western blot comparing the reactivity of the 6H6 anti-NS2 antibody and 9E10 anti-NSSA antibody against genotype 1a, 1b, and 2a proteins. Huh-7.5 cells were infected with a recombinant vaccinia helper virus expressing the T7 polymerase, followed by transfection with plasmids coding for a full-length HCV genomes under the control of a T7 promoter. The lysates were harvested 16 h posttransfection. The positions of molecular mass markers (in kilodaltons) are indicated to the right of the blot. (B) Amino acid sequence alignment of the 6H6 epitope region. Variation between protein sequences is indicated in red. (C) Crystal structure of the dimeric NS2 protease domain (21) with monomers shown in red and blue with the 6H6 antibody epitope shown in yellow.

pected, genomes containing a mutation of the NS5B RNA-dependent RNA polymerase motif GDD to GNN did not replicate (Fig. 1B and C).

**The monoclonal antibody 6H6 recognizes a C-terminal epitope of NS2.** In Western blot, MAb 6H6 strongly recognized NS2 from strains H77 (genotype 1a) and JFH-1 (Jc1 genome, genotype 2a) (16, 28) and showed a weak signal for strain J6 (J6/JFH genome, genotype 2a) (18); it did not react with Con1 (genotype 1b) (2) (Fig. 2A). Strain H77 NS2 is also recognized in an enzyme-linked immunosorbent assay, immunoprecipitation, and immunofluorescence (data not shown). Epitope mapping with an NS2 peptide library revealed that 6H6 binding occurs close to the NS2 C terminus (H77 NS2 amino acids 197 to 208, GQEILLGPADG). Sequence alignments in this region showed variability between NS2 genotypes that correlated with the Western blot results (Fig. 2B). The epitope of MAb 6H6 is shown on the NS2 crystal structure in Fig. 2C.

**NS2 catalytic-cleft residues are required for NS2-3 cleavage.** Previous studies have shown that the catalytic activity of the NS2-3 protease is not required for infectious virus production (14). To investigate whether residues surrounding the active site pocket were required for the generation of infectious prog-

eny, we mutated individual residues in this region. Y141 and L144 are highly conserved amino acids surrounding the protease active site, H143 is part of the catalytic triad, and P164 is an unusual *cis*-proline residue important for active site geometry. We mutated these residues to alanine and/or to less conservative substitutions in the context of the monocistronic J6/H77NS2/JFH and bicistronic J6/H77NS2/JFH(NS2-IRES-NS3) genome, and assayed replication by quantitative RT-PCR for intracellular HCV RNA at 72 h postelectroporation. We confirmed that the active site mutation H143A abolished replication in the full-length monocistronic background (10), and we found that Y141A also severely impaired RNA accumulation; a Y141F substitution, which preserved the aromatic ring, did not have a dramatic effect (Fig. 3A). Replication was decreased by mutation of L144 to bulky residues (L144F, L144K) and by substitutions of P164 (P164A, P164G). Consistent with the requirement for NS2-3 cleavage, robustly replicating genomes showed processed NS2 by Western blotting (Fig. 3C).

To test the effects of NS2 active cleft mutations on infectious virus production, we engineered these substitutions into the bicistronic J6/H77NS2/JFH(NS2-IRES-NS3) genome. In this context, all mutants replicated as efficiently as the wild-type virus did; J6/H77NS2/JFH(NS2-IRES-NS3)/GNN did not replicate (Fig. 3B). Infectious virus production was measured by inoculating naïve Huh-7.5 cells with filtered culture supernatants harvested at 72 h postelectroporation and calculating the TCID<sub>50</sub>/ml. Mutations Y141A, Y141F, H143A, L144F, and L144K were not impaired or only slightly impaired in terms of infectious titers compared to wild-type J6/H77NS2/JFH(NS2-IRES-NS3), whereas substitution of P164 mutated to Ala or Gly decreased infectious virus production by about 10-fold (Fig. 3D). Western blotting of cell lysates harvested at 72 h postelectroporation revealed that all of the mutants expressed readily detectable levels of NS2 (Fig. 3C).

These results indicate that mutations at the NS2 active cleft can inhibit replication of a monocistronic genome, likely by affecting NS2-3 processing, but that the catalytic activity is not required for infectious virus production of a bicistronic genome. The moderate deleterious effect of *cis*-proline 164 mutations on infectivity may indicate a more global impact of this unusual residue on NS2 architecture.

**Residues in the NS2 dimer crossover region are important for infectious virus production.** NS2 dimerization creates two composite active sites and has been shown to be essential for proteolytic cleavage at the NS2/NS3 junction (21). Although the critical residues for dimer formation and stabilization are not known, amino acids in the crossover region between the two monomers may be envisioned to participate. To test the effects of mutations in the dimer crossover region on replication and infectious virus production, we created several substitutions of highly conserved amino acids in the context of monocistronic and bicistronic genomes: a triple mutation with M170A, I175A, and W177A (M/I/W) and individual mutations M170A, I175S, W177A, and W177C. The single isoleucine-to-serine substitution was chosen in order to change a nonpolar residue to a polar residue, with predicted disruption to the dimer interface. In the monocistronic J6/H77NS2/JFH background, replication levels close to those of the wild type were observed for the M170A, I175S, and W177A mutants, whereas

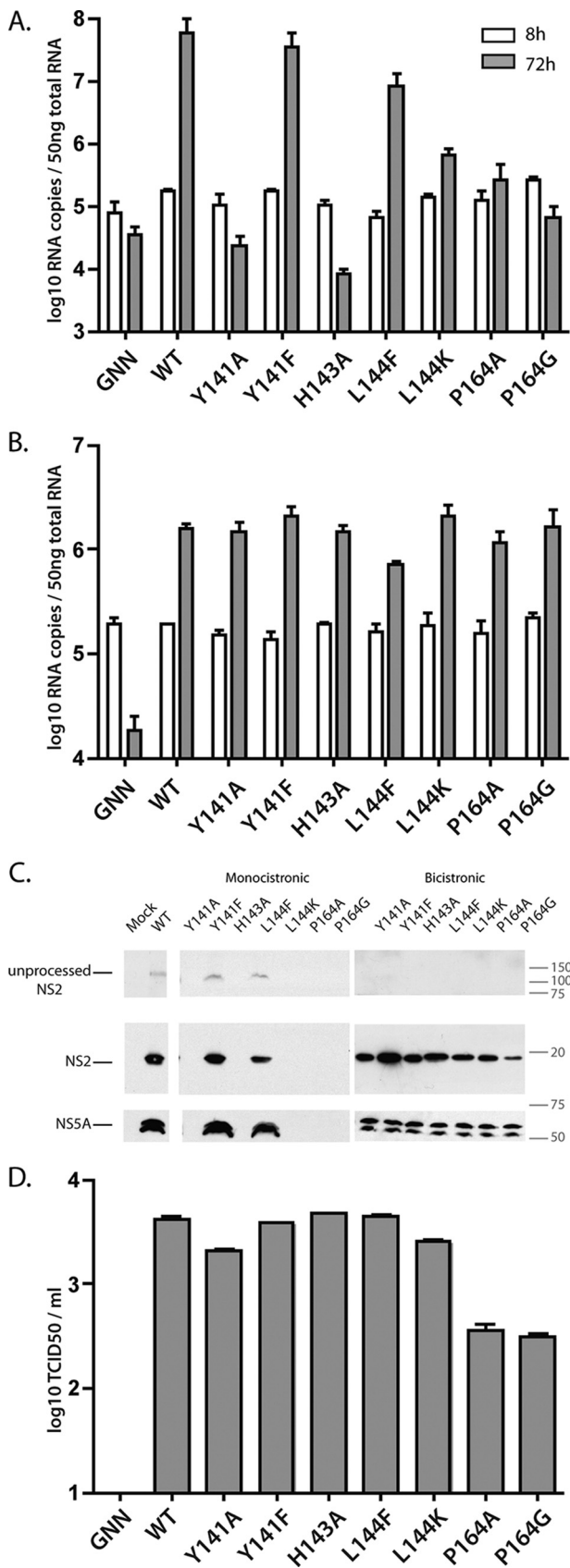


FIG. 3. Mutagenesis of the NS2 active site region. (A) RNA replication of GNN, the polymerase-defective control, wild-type (WT)

and the W177C mutant and the genome with the M/I/W triple mutation exhibited impaired RNA accumulation by 10- to 100-fold (Fig. 4A). This somewhat surprisingly efficient replication may indicate that dimer formation, and thereby protease activity, is not disrupted by these substitutions. Western blot analysis confirmed that NS2 was properly processed for each of these genomes, although to a lower extent for the triple mutant M/I/W (Fig. 4C). To test the effects of these mutations on infectious virus production, they were engineered into the bicistronic genome J6/H77NS2/JFH(NS2-IRES-NS3). While replication in this context was not affected by any of the NS2 substitutions (Fig. 4B), infectious particle production was decreased close to 100-fold for all of the mutant genomes (Fig. 4D). Wild-type levels of NS2 were detected for all the bicistronic constructs, indicating that the mutations do not change protein stability (Fig. 4C). These results indicate that mutations in the dimer crossover region are deleterious to infectious virus production, although likely not as a result of dimer destabilization.

**The C-terminal region of NS2 is essential for infectious virus production.** The crossover residues position the NS2 C-terminal region of one monomer close to the N-terminal region of the other, leading to the formation of the composite active site. To investigate the importance of the C-terminal region of NS2 for infectious virus production, we generated truncations after residues Y124, G137, G178, W214, R215, and L216 (Fig. 5A). These deletions were engineered in the context of the bicistronic *Gaussia* luciferase reporter genome, J6/H77NS2/JFH(NS2-IRES-nsGluc2AUBi), which was used to facilitate mutant characterization. Truncations were created by introducing two in-frame stop codons after the designated residue without deletion of the downstream nucleotides. This strategy allowed replication and infectivity to be monitored with minimal effects on genome length or potential RNA secondary structures. RNA replication was measured by assaying Huh-7.5 cell lysates for luciferase activity at 72 h postelectroporation. All the C-terminal truncation mutants replicated, although with a slight reduction for mutants with stops after G137 and G178 compared to wild type; J6/H77NS2/JFH(NS2-IRES-nsGluc2AUBi)/GNN did not replicate (Fig. 5B). Infectious virus production was assayed at 72 h postelectroporation by measuring luciferase activity in infected Huh-7.5 cell lysates.

and mutated monocistronic constructs at 8 h and 72 h postelectroporation. (B) RNA replication of GNN, wild-type and mutated bicistronic constructs at 8 h and 72 h postelectroporation. The numbers of HCV RNA copies per 50 ng of total cellular RNA are shown. (C) Polyprotein processing of monocistronic and bicistronic constructs. Huh-7.5 cells were lysed 72 h postelectroporation and analyzed by SDS-PAGE. Unprocessed and processed NS2 are shown in the top two panels (6H6 antibody). NS5A protein is shown in the bottom panel (9E10 antibody). The positions of molecular mass markers (in kilodaltons) are shown to the right of the immunoblots. (D) Infectious virus production by the bicistronic constructs at 72 h postelectroporation, as measured by limiting dilution assay (TCID<sub>50</sub>). Mutated residues are indicated (H77 NS2 numbering). WT and GNN, parental monocistronic or bicistronic wild type and polymerase-defective control, respectively. The means plus standard errors of the means (error bars) for three independent experiments with two different RNA preparations are shown.

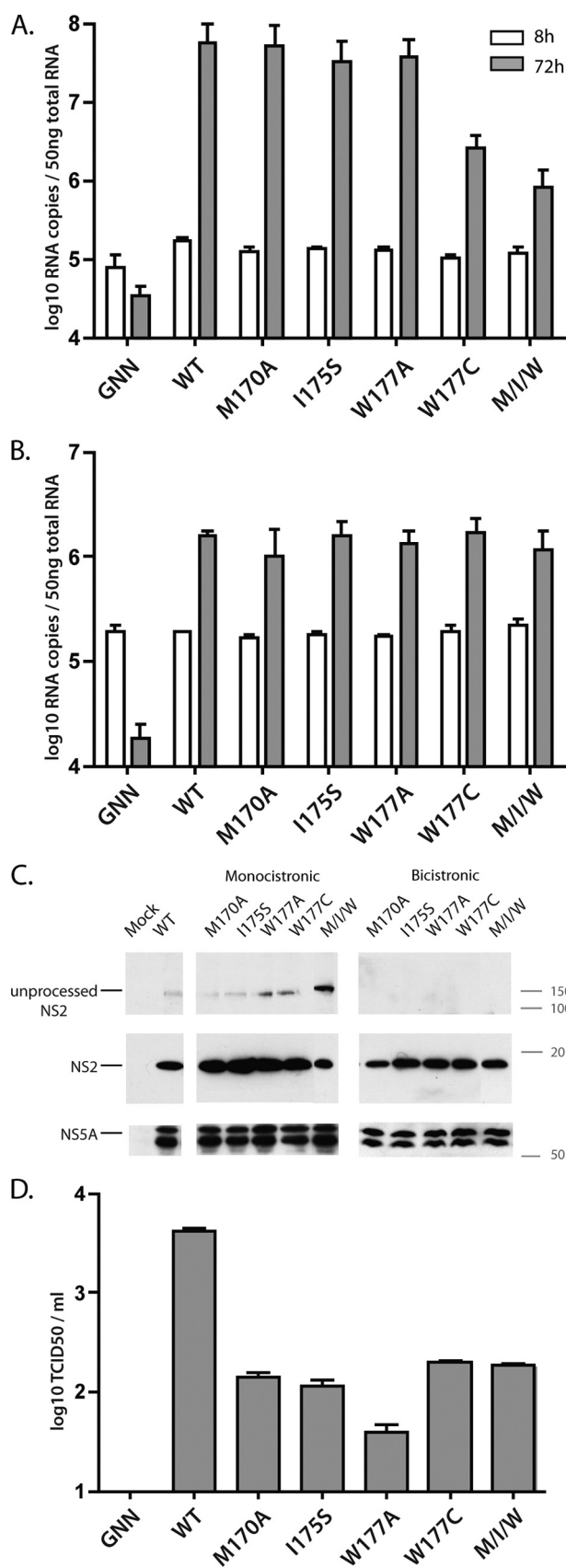


FIG. 4. Mutagenesis of the NS2 dimer crossover region. (A) RNA replication of GNN and wild-type and mutated monocistronic con-

structs at 8 h and 72 h postelectroporation. (B) RNA replication of bicistronic constructs at 8 h and 72 h postelectroporation. The numbers of HCV RNA copies per 50 ng of total cellular RNA are shown. (C) Polyprotein processing of monocistronic and bicistronic constructs. Huh-7.5 cells were lysed 72 h postelectroporation and analyzed by SDS-PAGE. Unprocessed and processed NS2 are shown in the top two panels (6H6 antibody). NS5A protein is shown in the bottom panel (9E10 antibody). The positions of molecular mass markers (in kilodaltons) are shown to the right of the immunoblots. (D) Infectious virus production by the bicistronic constructs at 72 h postelectroporation, as measured by limiting dilution assay (TCID<sub>50</sub>). Mutated residues are indicated (H77 NS2 numbering). WT and GNN, parental monocistronic or bicistronic wild type and polymerase-defective control, respectively. The means plus standard errors of the means (error bars) for three independent experiments with two different RNA preparations are shown.

Consistent with our mutational analysis (Fig. 4), truncation of NS2 before the dimer crossover region (Y124 and G137) abolished infectivity (Fig. 5C). Similarly, deletion of the entire C-terminal region (G178) prevented progeny virus production (Fig. 5C). Surprisingly, more subtle deletions of three, two, or even one amino acid from the C terminus severely impaired infectivity (Fig. 5C). Western blot analysis showed detectable levels of NS2 expression for the W214, R215, and L216 truncations (Fig. 5D); the larger deletions were missing the 6H6 antibody epitope and could therefore not be tested. To identify individual amino acids in the C-terminal region that were important for NS2 functions, we mutated highly conserved residues shown in the crystal structure to mediate contacts between NS2 monomers. These substitutions—non-polar I188 mutated to a polar serine, changing N189, L191, and I201 to a small amino acid (alanine), and changing D207 to alanine or a bulky, charged arginine—were created in the monocistronic J6/H77NS2/JFH and bicistronic J6/H77NS2/JFH(NS2-IRES-NS3) genomes. In the monocistronic background, RNA replication of the I188S, D207A, and D207R mutants was detected but impaired (Fig. 6A). NS2-3 processing could be observed for I188S, N189A, and L191A mutants; processing of the I201 and D207 mutants could not be assessed since the epitope of the 6H6 antibody had been disrupted (Fig. 6C). In the context of the bicistronic genome [J6/H77NS2/JFH(NS2-IRES-NS3)], none of the mutations in the C-terminal region impaired RNA replication (Fig. 6B). Infectious virus production was decreased for I188S, I201, D207A, and D207R mutants but not affected by N189A and L191S substitutions (Fig. 6D). The decreased titers seen for the I188S mutant did not result from NS2 degradation, as close to wild-type levels of this protein were detected by Western blotting.

Taken together, these results indicate that the C-terminal region of NS2 is important for infectious virus production, although individual residues contribute to various degrees. Interestingly, the ability of the mutations to disrupt replication of the monocistronic genome correlated with the extent of virus titer reduction, suggesting that attributes of the C-terminal region, such as interactions with the partner monomer, may be important for both proteolytic activity and infectious particle production.

**The C-terminal leucine of NS2 is critical for infectious virus production.** Our deletion analysis had shown that removing a

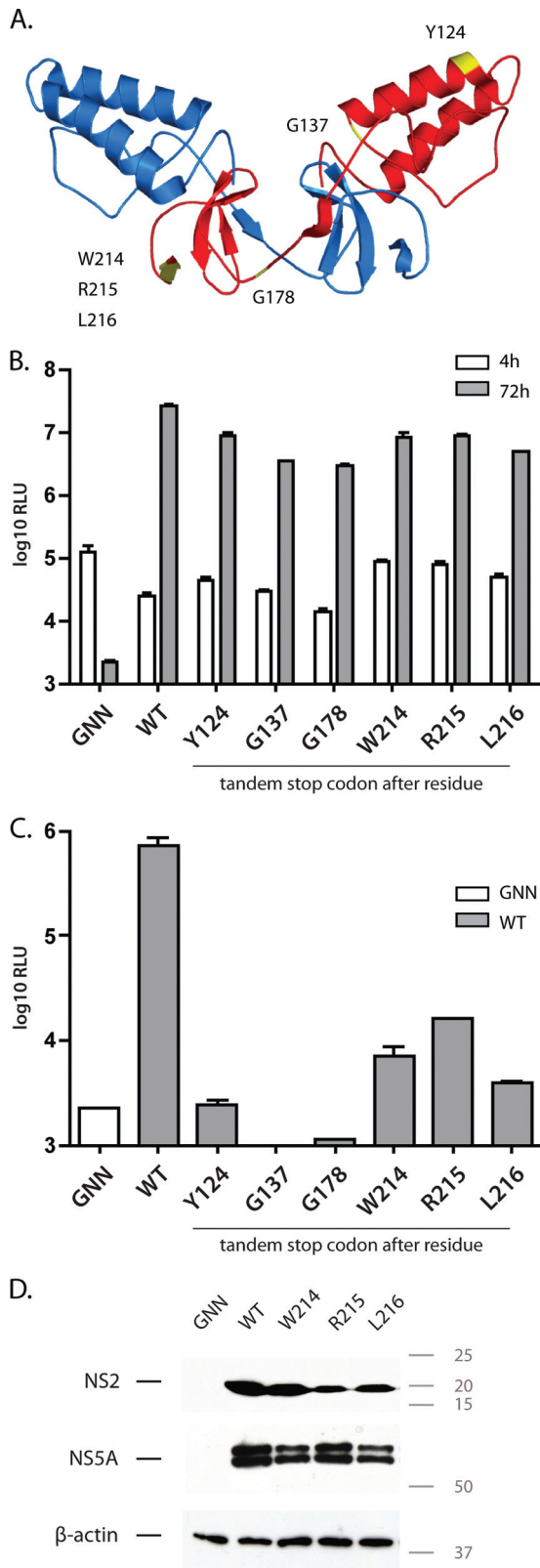


FIG. 5. Characterization of NS2 C-terminal truncations. (A) NS2<sup>PRO</sup> dimer with monomers shown in red and blue (21). The positions of the C-terminal truncations are indicated in yellow. (B) RNA replication at 4 h and 72 h postelectroporation of GNN, wild type, and C-terminal truncations in the bicistronic *Gaussia* luciferase reporter virus back-

ground, as measured by luciferase activity (in relative light units [RLU]). (C) Infectious virus production of NS2 C-terminal truncations at 72 h after infection of naive Huh-7.5 cells with supernatants harvested 72 h postelectroporation. Truncation points are indicated (H77 NS2 numbering). WT, wild type [J6/H77NS2/JFH(NS2-IRES-nsGluc2AUbi)]; GNN, J6/H77NS2/JFH(NS2-IRES-nsGluc2AUbi)/GNN. The means plus standard errors of the means (error bars) for three independent experiments with two different RNA preparations are shown. (D) Polyprotein processing of NS2 truncations. Huh-7.5 cells lysed 72 h postelectroporation and analyzed by SDS-PAGE. NS2 expression is shown in the top panel (6H6 antibody), NS5A protein in the middle panel (9E10 antibody), and  $\beta$ -actin control in the bottom. The antibody epitope is not present in the NS2 truncations Y124, G137, and G178. The positions of molecular mass markers (in kilodaltons) are shown to the right of the immunoblots.

single NS2 residue, the C-terminal leucine 217, almost completely abolished infectious virus production. The crystal structure of the postcleavage form of NS2<sup>PRO</sup> shows that leucine 217 remains in the active site through hydrogen bond interactions with the catalytic triad, a conformation that is proposed to limit the enzyme to a single autoproteolytic cleavage (21). To investigate the importance of this C-terminal residue for infectivity, L217 was mutated to a variety of amino acids— isoleucine, valine, alanine, tryptophan, asparagine, or lysine—in the context of the bicistronic reporter virus, J6/H77NS2/JFH(NS2-IRES-nsGluc2AUbi). The L217 mutants replicated, although at levels somewhat reduced compared to that of the wild type (Fig. 7A). Infectious virus production was markedly impaired for all mutants tested apart from L217I, which showed a reduction of infectious titers of about 10-fold (Fig. 7B). These defects were not a result of NS2 instability, as the mutant proteins were readily detected by Western blotting (Fig. 7C). These data suggest that infectious virus production specifically requires a leucine at the C terminus of NS2, although an isoleucine can function to some degree.

**Additional residues fused to the C terminus of NS2 abolish infectious virus production.** NS2 requires residues 1 to 181 of NS3 for optimal proteolytic activity (30). Our finding of a critical role for the NS2 C-terminal leucine in infectivity suggested divergent requirements for infectious virus production and proteolysis. To investigate the effect of adding residues from NS3 on viral titers, we created J6/H77NS2/JFH bicistronic reporter genomes in which NS2 was followed by 1, 31, 40, 90, or 181 amino acids of NS3, a stop codon, the EMCV IRES, the *Gaussia* luciferase-2AUbi cassette, and full-length NS3 (Fig. 8A). These extensions were created in the context of wild-type H77 NS2, as well as in the context of the H143A active site mutation to prevent NS2-3 cleavage. At 72 h post-electroporation, the NS3 fusion constructs replicated, although extensions of 1, 31, 40, and 90 amino acids impaired this process up to 10-fold, in both the wild-type and H143A backgrounds. Mutant virus with the 181-amino-acid extension showed replication levels comparable to that of the parental genome in the wild-type background but more drastically impaired RNA replication in the H143A background; the reasons for this discrepancy are not known (Fig. 8B). Infectious virus production was severely impaired by uncleavable NS3 fusions of 31 to 181 amino acids (Fig. 8C). Even the addition of a single NS3 residue decreased infectivity by three- to fivefold. In

ground, as measured by luciferase activity (in relative light units [RLU]). (C) Infectious virus production of NS2 C-terminal truncations at 72 h after infection of naive Huh-7.5 cells with supernatants harvested 72 h postelectroporation. Truncation points are indicated (H77 NS2 numbering). WT, wild type [J6/H77NS2/JFH(NS2-IRES-nsGluc2AUbi)]; GNN, J6/H77NS2/JFH(NS2-IRES-nsGluc2AUbi)/GNN. The means plus standard errors of the means (error bars) for three independent experiments with two different RNA preparations are shown. (D) Polyprotein processing of NS2 truncations. Huh-7.5 cells lysed 72 h postelectroporation and analyzed by SDS-PAGE. NS2 expression is shown in the top panel (6H6 antibody), NS5A protein in the middle panel (9E10 antibody), and  $\beta$ -actin control in the bottom. The antibody epitope is not present in the NS2 truncations Y124, G137, and G178. The positions of molecular mass markers (in kilodaltons) are shown to the right of the immunoblots.

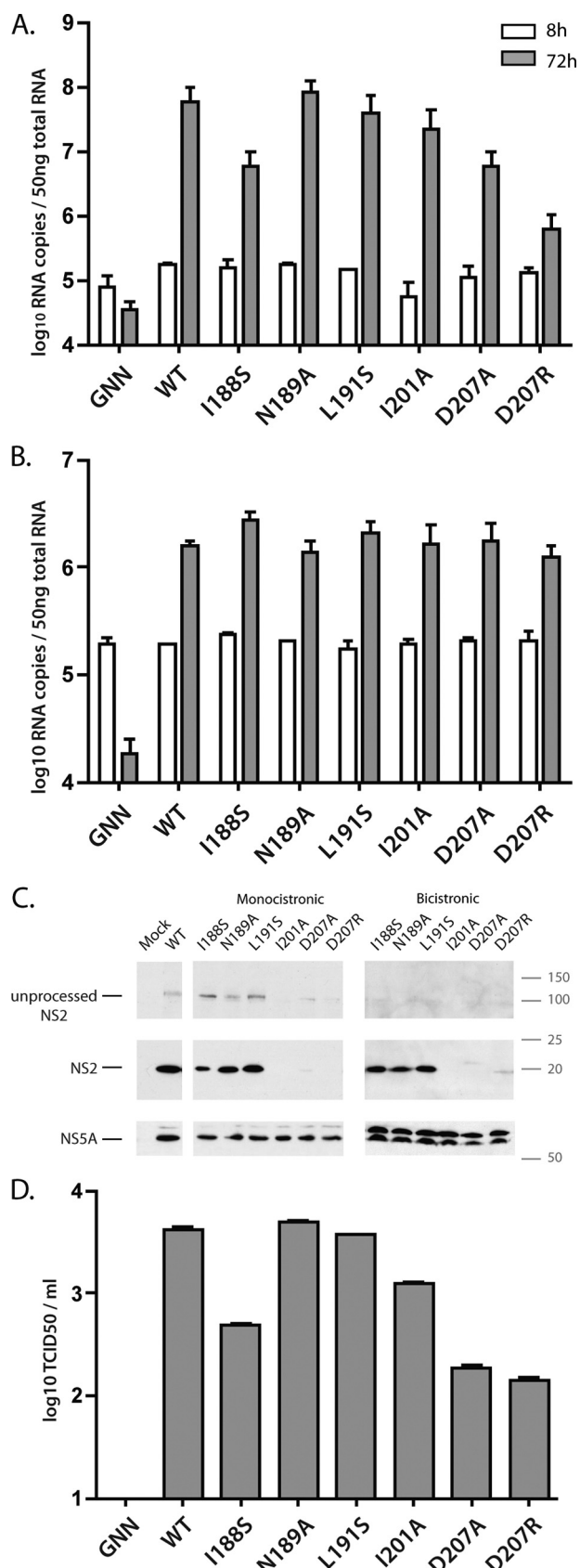


FIG. 6. Mutagenesis of the NS2 C-terminal region. (A) RNA replication of GNN and wild-type and mutated monocistronic constructs

the context of wild-type, but not protease-defective NS2, fusion of 181 amino acids of NS3 produced infectious virus, suggesting that productive NS2-3 cleavage was required. Analysis of protein expression and processing by Western blotting indicated the presence of processed NS2 for those genomes producing significant levels of infectivity (Fig. 8D). Interestingly and consistent with the recent results of Schregel et al. (33), a small portion of processed NS2 could be detected for fusions expressing 31 and 40 amino acids of NS3. Taken together, these results further demonstrate the importance of the C-terminal residue of NS2 in infectious virus production and add to accumulating evidence that the multiple roles of NS2 in the viral life cycle have contrasting protein determinants.

### DISCUSSION

NS2 has an essential but mechanistically undefined role in infectious HCV assembly (14, 28). The first set of determinants for this activity have been mapped; essential residues were identified in the N-terminal transmembrane domains, and a catalysis-independent role for the protease was found (13, 14). Here, we investigated the determinants of the NS2 protease domain that are required for infectious particle production. On the basis of the NS2<sup>Pro</sup> crystal structure (21) and sequence alignments, conserved features of the various structural regions were analyzed. We found that most point mutations around the active site had little effect on infectious virus production but indirectly affected RNA replication in the context of a monocistronic genome, most likely by preventing NS2-3 cleavage. In contrast, mutations in the dimer crossover region and the C-terminal domain impaired or abolished infectious virus production. In addition, we showed the importance of a properly cleaved C terminus of NS2 with a free leucine 217.

The catalytic activity of the NS2 protease is required for NS2-3 processing (16, 38), but not for infectious virus assembly (14). In addition to the catalytic histidine, we identified several other residues important for NS2-3 processing and replication of a monocistronic genome. Mutation of Y141 to Ala abolished NS2-3 cleavage, whereas a more conservative change to Phe had little effect on processing or replication. The aromatic ring of position 141 acts as a support for the active site, a function that likely cannot tolerate a smaller side chain. Leucine 144 performs a similar role in creating the correct active site architecture, but we found that mutation of this

at 8 h and 72 h postelectroporation. (B) RNA replication of the bicistronic constructs at 8 h and 72 h postelectroporation. The numbers of HCV RNA copies per 50 ng of total cellular RNA are shown. (C) Polyprotein processing of monocistronic and bicistronic constructs. Huh-7.5 cells were lysed 72 h postelectroporation and analyzed by SDS-PAGE. Unprocessed and processed NS2 are shown in the top two panels (6H6 antibody). NS5A protein is shown in the bottom panel (9E10 antibody). The positions of molecular mass markers (in kilodaltons) are shown to the right of the immunoblots. (D) Infectious virus production at 72 h postelectroporation, as measured by limiting dilution assay (TCID<sub>50</sub>). Mutated residues are indicated (H77 NS2 numbering). WT and GNN, parental monocistronic or bicistronic wild type and polymerase-defective control, respectively. The means plus standard errors of the means (error bars) for three independent experiments with two different RNA preparations are shown.



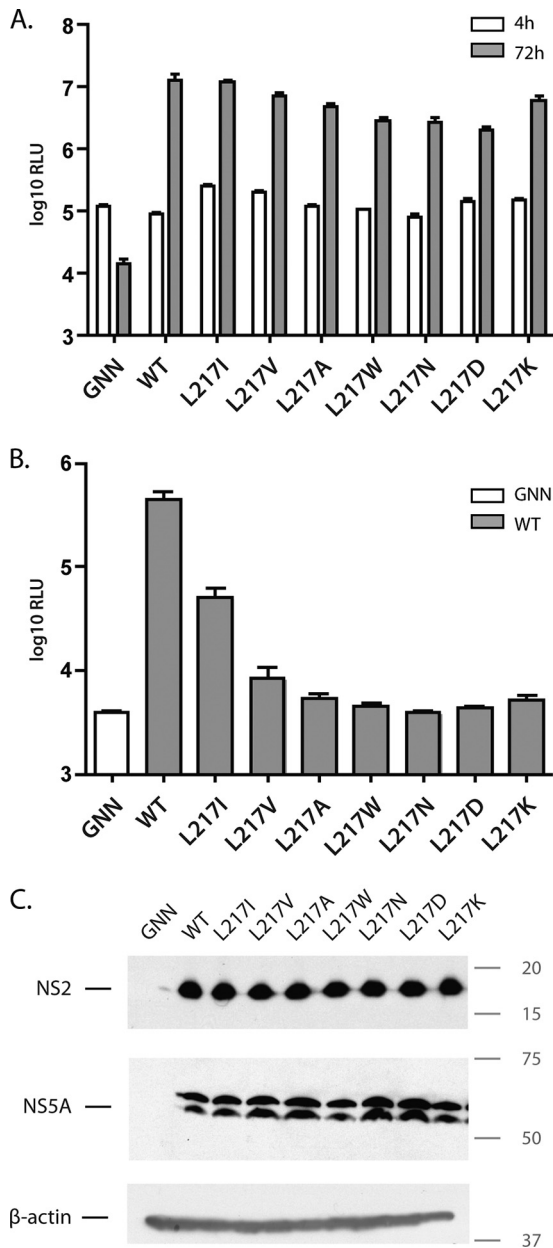
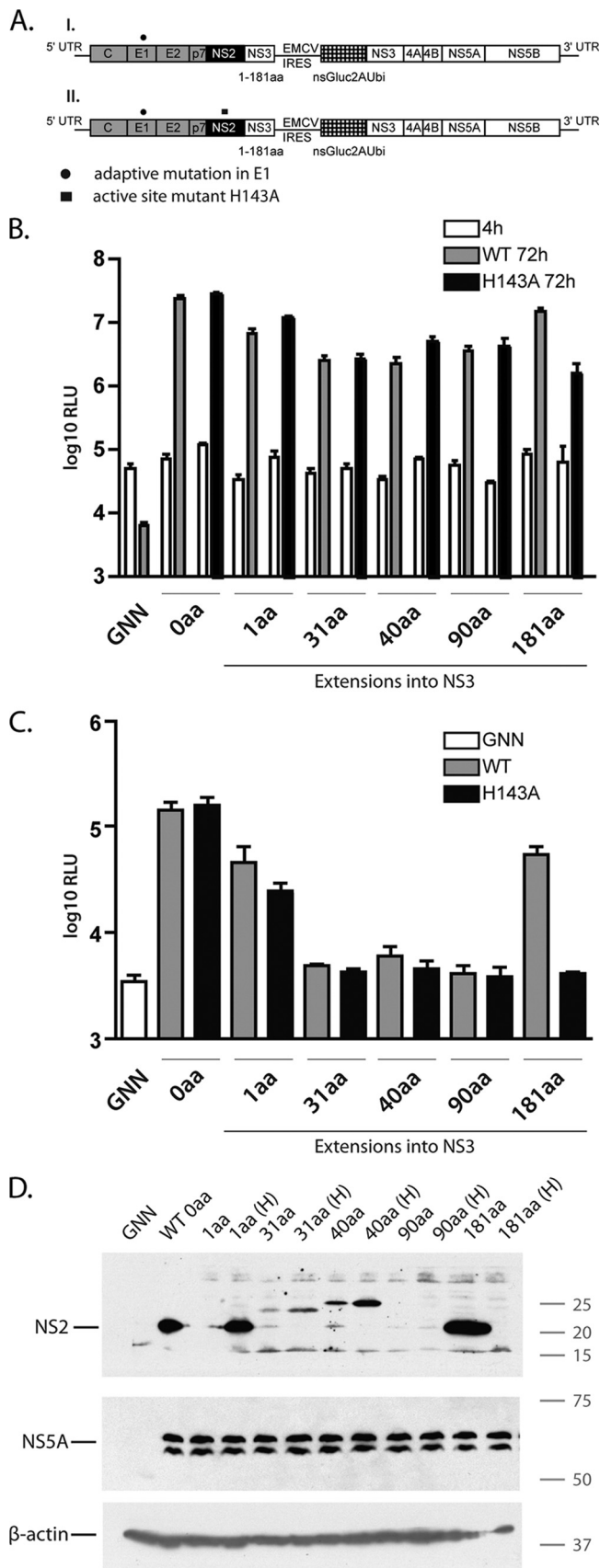


FIG. 7. Mutagenesis of the NS2 C-terminal leucine 217. (A) RNA replication at 4 h and 72 h postelectroporation of GNN, wild type, and C-terminal mutants in the context of the bicistronic *Gaussia* luciferase reporter virus, as measured by luciferase activity (in relative light units [RLU]). (B) Infectious virus production of genomes bearing Leu 217 mutations at 72 h after infection of naïve Huh-7.5 cells with supernatants harvested 72 h postelectroporation. WT, wild type [J6/H77NS2/JFH(NS2-IRES-nsGluc2AUbi)]; GNN, J6/H77NS2/JFH(NS2-IRES-nsGluc2AUbi)/GNN. The means plus standard errors of the means (error bars) for three independent experiments with two different RNA preparations are shown. (C) Polyprotein processing of 72 h postelectroporation. Huh-7.5 cells were lysed and analyzed by SDS-PAGE. NS2 expression is shown in the top panel (6H6 antibody), NS5A protein in the middle panel (9E10 antibody), and  $\beta$ -actin control in the bottom. The positions of molecular mass markers (in kilodaltons) are shown to the right of the immunoblots.

residue to Phe allowed detectable levels of NS2-3 processing, whereas Lys apparently abolished the function of the active site. Proline 164 has a *cis* conformation that is thought to bend the peptide backbone to establish the correct geometry of the Glu 163 side chain for catalysis; mutation of P164 to Ala or Gly prevented replication of a monocistronic genome. The majority of active site changes had little effect on infectious virus production in a bicistronic genome. Substitutions of P164, however, decreased infectious titers. It is possible that mutation of this *cis*-proline dramatically affects NS2 structure; indeed, the P164G substitution appeared to slightly destabilize the protein. It is also possible that mutations of P164 affect NS2 dimer formation, as this proline is important for positioning the linker between the N- and C-terminal subdomains. Alternatively, P164 may directly participate in infectious virus assembly independent of a role in catalysis. Studies of the NS2-3 protein of the distantly related pestivirus, classical swine fever virus, have similarly shown that the NS2 protease activity is dispensable for infectious virus production (23). However, a histidine-to-arginine mutation within the active site abolished infectivity without affecting NS2-3 expression (23).

The crystal structure of NS2<sup>pro</sup> shows a crossover region that positions the subdomains for creation of the composite active sites (21). We hypothesized that mutations in this region would disrupt dimer stability and NS2-3 processing. RNA replication of a monocistronic genome, however, was impaired only by substitution of W177 to Cys or by a triple mutation of M170A/I175A/W177A. This suggests that single point mutations do not have a drastic effect on dimer integrity; indeed, the significant buried surface area between the monomers indicates that the NS2 dimer is highly stable (21). Although NS2-3 processing was not greatly impacted by mutations in the crossover sequence, infectious virus production was impaired by all substitutions we tested in this region. A number of the crossover residues are exposed on the surface of the NS2<sup>pro</sup> dimer (Fig. 9). Mutations in this region may disrupt associations with viral or host proteins involved in infectious virus production. Indeed, NS2 has been suggested to participate in a number of genetic or physical interactions, including with structural proteins core and E2 as well as with nonstructural proteins p7, NS3, NS4A, and NS5A (15, 19, 25, 29, 34, 40). The A269T adaptive mutation identified here suggests a genetic interaction between NS2 and E1. Cellular kinase CKII also appears to associate with and phosphorylate NS2 (8), and NS2 may interact with additional host factors to influence apoptosis (6) and cellular gene expression (5).

In addition to mediating contacts between monomers, the C-terminal subdomain of NS2 contributes the catalytic cysteine to the composite active site. Deletion analysis revealed that even a single amino acid truncation at the C terminus severely impaired infectious virus production. Furthermore, the majority of substitutions at the terminal L217 were highly deleterious to infectivity. Interestingly, previous reports have shown that most modifications of L217 have little effect on NS2-3 processing (12, 30). Our finding of an essential role for L217 in infectious virus production helps explain its high level of conservation across all genotypes. The structure of the postcleavage form of NS2<sup>pro</sup> shows that L217 occupies the active site through contacts with H143 and C184 (13, 21). This conformation has been suggested to render the protease inactive



after a single autoproteolytic processing event (21). Although NS2 expression and stability were not dramatically altered by most C-terminal substitutions, it is possible that deletion of L217 changes the structure of NS2 by liberating the C terminus from the active site. Releasing the C terminus might alter the position of the C-terminal subdomain, affecting surfaces required for essential interactions, such as dimerization or heterotypic associations with viral or host proteins. A similar function of a C-terminal residue is seen for the alphavirus capsid protein, which is also an autoprotease involved in infectious virus assembly. Analogous to NS2, the highly conserved C-terminal tryptophan of the alphavirus capsid occupies the active site postcleavage (4); in fact, distinct similarities have been noted in the catalytic cleft architecture of the two enzymes (21). Mutation of this C-terminal tryptophan to alanine or arginine in a system that uncoupled proteolysis from infectious alphavirus production almost completely abolished nucleocapsid assembly; substitution of the terminal tryptophan with phenylalanine, however, was tolerated (35). Similarly, mutations in the alphavirus capsid that displaced the terminal tryptophan from the active site pocket were found to be highly deleterious to its function (3). These observations suggest that the location of the C terminus, as well as the presence of a leucine or similar residue at position 217, may be critical to the structure and postcleavage functions of these viral proteases.

Further supporting the critical role for L217 in infectious virus production, we found that C-terminal extensions into NS3 were highly deleterious; even one additional amino acid reduced viral titers by three to fivefold. Similar results have been previously reported, where ubiquitin fused to the NS2 C terminus abolished infectious virus production (13). Interestingly, we observed that extensions shorter than the minimal functional NS3 protease domain (31, 40, and 90 amino acids) showed NS2-3 processing to some extent in the context of a functional NS2 active site; recent work from Schregel et al. has similarly demonstrated residual enzymatic activity of NS2 followed by only 2 amino acids of NS3 (33). Despite detectable

FIG. 8. Characterization of NS2 C-terminal extensions. (A) Schematic representation of J6/H77NS2/JFH(NS3\*-IRES-nsGluc2AUbiNS3). Genes from J6 (core-p7) (gray boxes), H77 (NS2) (black boxes), and from JFH (white boxes) are indicated. This construct contains JFH NS3 extensions of 1, 31, 40, 90, or 181 amino acids, followed by an EMCV IRES, a *Gaussia* luciferase cassette (nsGluc2AUbi), and JFH nonstructural proteins NS3-NS5B. Wild-type H77 NS2 (I) and H77 NS2 encoding active-site mutation H143A (small solid square) (II). 5' UTR and 3'UTR, 5' untranslated region and 3' untranslated region, respectively. (B) RNA replication at 4 h postelectroporation, 72 h postelectroporation for the wild type, and 72 h postelectroporation for H143A as measured by luciferase activity (in relative light units [RLU]). 0aa, 0 amino acid. (C) Infectious virus production at 72 h postelectroporation, as measured by luciferase activity in infected cells. GNN, replication-deficient control, WT, wild-type NS2 protease; H143A, cleavage-deficient NS2 protease. The means plus standard errors of the means (error bars) for three independent experiments with two different RNA preparations are shown. (D) NS2 protein expression at 72 h postelectroporation of either wild-type or cleavage-deficient (H) NS3 extension constructs. Top panel NS2 (6H6 antibody), NS5A protein in the middle panel (9E10 antibody), and  $\beta$ -actin control in the bottom. GNN, corresponding polymerase-defective control of wild-type NS2. The positions of molecular mass markers (in kilodaltons) are indicated to the right of the immunoblots.

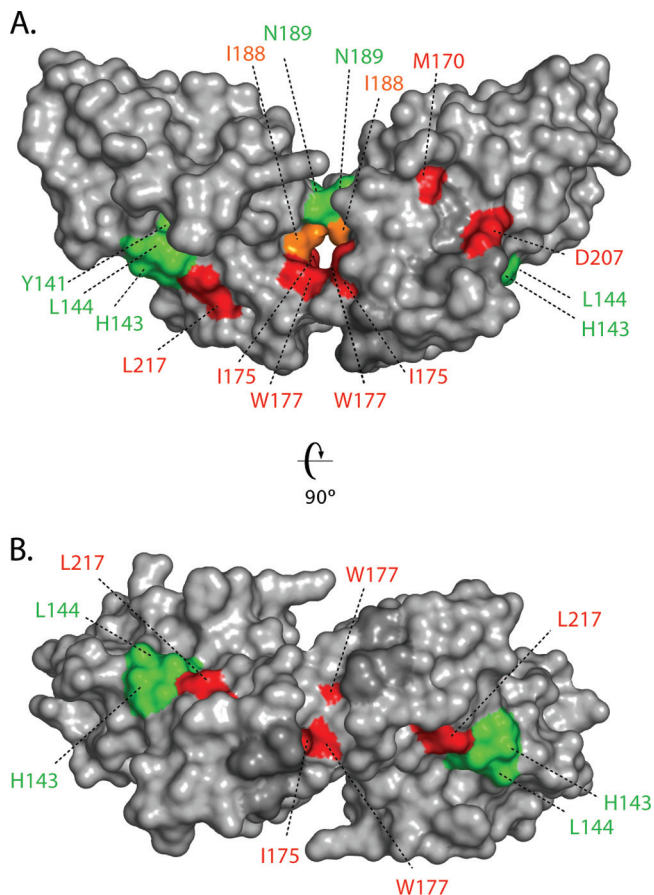


FIG. 9. Summary of critical NS2<sup>pro</sup> residues. (A) Exposed surface rendering of the NS2<sup>pro</sup> dimer. Mutations showing abolished infectious virus production are shown in red (M170, I175, W177, D207, and L217), mutations showing impaired infectious virus production are shown in orange (P164 and I188), and mutations with no significant effect on infectious virus production are shown in green (Y141, H143, L144, N189, and L191). (B) NS2<sup>pro</sup> dimer rotated 90° around the horizontal axis as shown in panel A.

NS2-3 processing, however, genomes encoding NS3 extensions still did not support infectious virus production. This could indicate that insufficient quantities of mature NS2 are produced by suboptimal cleavage or that short fragments of NS3 impair infectivity, possibly by acting as dominant-negative inhibitors of interactions between NS2 and full-length NS3 (15). The finding that fused residues from NS3 are deleterious to the role of HCV NS2 infectivity contrasts with the related pestiviruses, in which the uncleaved NS2-3 precursor is essential for infectious virus production (1, 23). The possibility that NS2 and NS3 form functional associations during virion morphogenesis, however, suggests conserved strategies between HCV and other members of the family *Flaviviridae* (24).

Using monocistronic and bicistronic genomes, we were able to analyze the effects of NS2 mutations on protease activity and postcleavage functions. Our results add to accumulating evidence that the determinants of these two essential roles are divergent. Previous work has demonstrated that the transmembrane domains of NS2 play critical roles in infectivity (13) but are not absolutely required for protease activity (10, 26, 32, 37).

Conversely, the active cleft is essential for the protease function but predominantly dispensable for infectivity (13, 14; this study). A number of substitutions in the dimer crossover region and C-terminal subdomain affected infectious titers, but not protease activity, and L217 was found to be dispensable for processing but critical for infectious virus production. Similarly, the finding that NS2 functions in assembly do not tolerate C-terminal extensions contrasts with the requirement for the NS3 protease domain for optimal NS2-3 cleavage. These differences highlight the two distinct functions of NS2 and suggest that further analysis of these roles may reveal important regulatory switches.

In conclusion, we dissected the determinants of the NS2 protease domain required for infectious virus production. We found critical roles for residues in the dimer crossover region and at the extreme C terminus of the protein, and we showed that C-terminal extensions into NS3 are deleterious to infectivity. These insights increase our understanding of the multifunctional NS2 protein and may facilitate exploiting this target for antiviral drug development.

#### ACKNOWLEDGMENTS

We thank Maryline Panis and Anesta Webson for laboratory support and technical assistance. We are grateful to Catherine L. Murray, Christopher T. Jones, Cynthia de la Fuente, and Kimberly D. Ritola for reagents, constructs, helpful discussions, and critical reading of the manuscript.

This study was supported by The Greenberg Medical Research Institute, NIH Public Health Service grant (AI075099), and the Starr Foundation. T.G.D. is supported by the Fonds National de la Recherche Luxembourg.

#### REFERENCES

- Agapov, E. V., C. L. Murray, I. Frolov, L. Qu, T. M. Myers, and C. M. Rice. 2004. Uncleaved NS2-3 is required for production of infectious bovine viral diarrhoea virus. *J. Virol.* **78**:2414–2425.
- Blight, K. J., J. A. McKeating, and C. M. Rice. 2002. Highly permissive cell lines for subgenomic and genomic hepatitis C virus RNA replication. *J. Virol.* **76**:13001–13014.
- Choi, H. K., S. Lee, Y. P. Zhang, B. R. McKinney, G. Wengler, M. G. Rossmann, and R. J. Kuhn. 1996. Structural analysis of Sindbis virus capsid mutants involving assembly and catalysis. *J. Mol. Biol.* **262**:151–167.
- Choi, H. K., L. Tong, W. Minor, P. Dumas, U. Boege, M. G. Rossmann, and G. Wengler. 1991. Structure of Sindbis virus core protein reveals a chymotrypsin-like serine proteinase and the organization of the virion. *Nature* **354**:37–43.
- Dumoulin, F. L., A. von dem Bussche, J. Li, L. Khamzina, J. R. Wands, T. Sauerbruch, and U. Spengler. 2003. Hepatitis C virus NS2 protein inhibits gene expression from different cellular and viral promoters in hepatic and nonhepatic cell lines. *Virology* **305**:260–266.
- Erdtmann, L., N. Franck, H. Lerat, J. Le Seyec, D. Gilot, I. Cannie, P. Gripon, U. Hibner, and C. Guguen-Guillouzo. 2003. The hepatitis C virus NS2 protein is an inhibitor of CIDE-B-induced apoptosis. *J. Biol. Chem.* **278**:18256–18264.
- Everhart, J. E., Y. Wei, H. Eng, M. R. Charlton, D. H. Persing, R. H. Wiesner, J. J. Germer, J. R. Lake, R. K. Zetterman, and J. H. Hoofnagle. 1999. Recurrent and new hepatitis C virus infection after liver transplantation. *Hepatology* **29**:1220–1226.
- Franck, N., J. Le Seyec, C. Guguen-Guillouzo, and L. Erdtmann. 2005. Hepatitis C virus NS2 protein is phosphorylated by the protein kinase CK2 and targeted for degradation to the proteasome. *J. Virol.* **79**:2700–2708.
- Grakoui, A., D. W. McCourt, C. Wychowski, S. M. Feinstone, and C. M. Rice. 1993. A second hepatitis C virus-encoded proteinase. *Proc. Natl. Acad. Sci. USA* **90**:10583–10587.
- Grakoui, A., D. W. McCourt, C. Wychowski, S. M. Feinstone, and C. M. Rice. 1993. Characterization of the hepatitis C virus-encoded serine proteinase: determination of proteinase-dependent polyprotein cleavage sites. *J. Virol.* **67**:2832–2843.
- Hijikata, M., H. Mizushima, T. Akagi, S. Mori, N. Kakiuchi, N. Kato, T. Tanaka, K. Kimura, and K. Shimotohno. 1993. Two distinct proteinase activities required for the processing of a putative nonstructural precursor protein of hepatitis C virus. *J. Virol.* **67**:4665–4675.

12. Hirowatari, Y., M. Hijikata, Y. Tanji, H. Nyunoya, H. Mizushima, K. Kimura, T. Tanaka, N. Kato, and K. Shimotohno. 1993. Two proteinase activities in HCV polypeptide expressed in insect cells using baculovirus vector. *Arch. Virol.* **133**:349–356.
13. Jirasko, V., R. Montserret, N. Appel, A. Janvier, L. Eustachi, C. Brohm, E. Steinmann, T. Pietschmann, F. Penin, and R. Bartenschlager. 2008. Structural and functional characterization of nonstructural protein 2 for its role in hepatitis C virus assembly. *J. Biol. Chem.* **283**:28546–28562.
14. Jones, C. T., C. L. Murray, D. K. Eastman, J. Tassello, and C. M. Rice. 2007. Hepatitis C virus p7 and NS2 proteins are essential for production of infectious virus. *J. Virol.* **81**:8374–8383.
15. Kiiver, K., A. Merits, M. Ustav, and E. Zusinaite. 2006. Complex formation between hepatitis C virus NS2 and NS3 proteins. *Virus Res.* **117**:264–272.
16. Kolykhalov, A. A., E. V. Agapov, K. J. Blight, K. Mihalik, S. M. Feinstone, and C. M. Rice. 1997. Transmission of hepatitis C by intrahepatic inoculation with transcribed RNA. *Science* **277**:570–574.
17. Liang, T. J., B. Rehermann, L. B. Seeff, and J. H. Hoofnagle. 2000. Pathogenesis, natural history, treatment, and prevention of hepatitis C. *Ann. Intern. Med.* **132**:296–305.
18. Lindenbach, B. D., M. J. Evans, A. J. Syder, B. Wolk, T. L. Tellinghuisen, C. C. Liu, T. Maruyama, R. O. Hynes, D. R. Burton, J. A. McKeating, and C. M. Rice. 2005. Complete replication of hepatitis C virus in cell culture. *Science* **309**:623–626.
19. Liu, Q., R. A. Bhat, A. M. Prince, and P. Zhang. 1999. The hepatitis C virus NS2 protein generated by NS2-3 autocleavage is required for NS5A phosphorylation. *Biochem. Biophys. Res. Commun.* **254**:572–577.
20. Lohmann, V., F. Korner, J. Koch, U. Herian, L. Theilmann, and R. Bartenschlager. 1999. Replication of subgenomic hepatitis C virus RNAs in a hepatoma cell line. *Science* **285**:110–113.
21. Lorenz, I. C., J. Marcotrigiano, T. G. Dentzer, and C. M. Rice. 2006. Structure of the catalytic domain of the hepatitis C virus NS2-3 protease. *Nature* **442**:831–835.
22. Moradpour, D., F. Penin, and C. M. Rice. 2007. Replication of hepatitis C virus. *Nat. Rev. Microbiol.* **5**:453–463.
23. Moulin, H. R., T. Seuberlich, O. Bauhofer, L. C. Bennett, J. D. Tratschin, M. A. Hofmann, and N. Ruggli. 2007. Nonstructural proteins NS2-3 and NS4A of classical swine fever virus: essential features for infectious particle formation. *Virology* **365**:376–389.
24. Murray, C. L., C. T. Jones, and C. M. Rice. 2008. Architects of assembly: roles of Flaviviridae non-structural proteins in virion morphogenesis. *Nat. Rev. Microbiol.* **6**:699–708.
25. Murray, C. L., C. T. Jones, J. Tassello, and C. M. Rice. 2007. Alanine scanning of the hepatitis C virus core protein reveals numerous residues essential for production of infectious virus. *J. Virol.* **81**:10220–10231.
26. Pallaoro, M., A. Lahm, G. Biasiol, M. Brunetti, C. Nardella, L. Orsatti, F. Bonelli, S. Orru, F. Narjes, and C. Steinkuhler. 2001. Characterization of the hepatitis C virus NS2/3 processing reaction by using a purified precursor protein. *J. Virol.* **75**:9939–9946.
27. Penin, F., J. Dubuisson, F. A. Rey, D. Moradpour, and J. M. Pawlotsky. 2004. Structural biology of hepatitis C virus. *Hepatology* **39**:5–19.
28. Pietschmann, T., A. Kaul, G. Koutsoudakis, A. Shavinskaya, S. Kallis, E. Steinmann, K. Abid, F. Negro, M. Dreux, F. L. Cosset, and R. Bartenschlager. 2006. Construction and characterization of infectious intragenotypic and intergenotypic hepatitis C virus chimeras. *Proc. Natl. Acad. Sci. USA* **103**:7408–7413.
29. Pietschmann, T., V. Lohmann, A. Kaul, N. Krieger, G. Rinck, G. Rutter, D. Strand, and R. Bartenschlager. 2002. Persistent and transient replication of full-length hepatitis C virus genomes in cell culture. *J. Virol.* **76**:4008–4021.
30. Reed, K. E., A. Grakoui, and C. M. Rice. 1995. Hepatitis C virus-encoded NS2-3 protease: cleavage-site mutagenesis and requirements for bimolecular cleavage. *J. Virol.* **69**:4127–4136.
31. Ryan, M. D., A. M. King, and G. P. Thomas. 1991. Cleavage of foot-and-mouth disease virus polyprotein is mediated by residues located within a 19 amino acid sequence. *J. Gen. Virol.* **72**:2727–2732.
32. Santolini, E., L. Pacini, C. Fipaldini, G. Migliaccio, and N. Monica. 1995. The NS2 protein of hepatitis C virus is a transmembrane polypeptide. *J. Virol.* **69**:7461–7471.
33. Schregel, V., S. Jacobi, F. Penin, and N. Tautz. 2009. Hepatitis C virus NS2 is a protease stimulated by cofactor domains in NS3. *Proc. Natl. Acad. Sci. USA* **106**:5342–5347.
34. Selby, M. J., E. Glazer, F. Masiarz, and M. Houghton. 1994. Complex processing and protein:protein interactions in the E2:NS2 region of HCV. *Virology* **204**:114–122.
35. Skoging, U., and P. Liljestrom. 1998. Role of the C-terminal tryptophan residue for the structure-function of the alphavirus capsid protein. *J. Mol. Biol.* **279**:865–872.
36. Steinmann, E., F. Penin, S. Kallis, A. H. Patel, R. Bartenschlager, and T. Pietschmann. 2007. Hepatitis C virus p7 protein is crucial for assembly and release of infectious virions. *PLoS Pathog.* **3**:e103.
37. Thibeault, D., R. Maurice, L. Pilote, D. Lamarre, and A. Pause. 2001. In vitro characterization of a purified NS2/3 protease variant of hepatitis C virus. *J. Biol. Chem.* **276**:46678–46684.
38. Welbourn, S., R. Green, I. Gamache, S. Dandache, V. Lohmann, R. Bartenschlager, K. Meerovitch, and A. Pause. 2005. Hepatitis C virus NS2/3 processing is required for NS3 stability and viral RNA replication. *J. Biol. Chem.* **280**:29604–29611.
39. Yamaga, A. K., and J. H. Ou. 2002. Membrane topology of the hepatitis C virus NS2 protein. *J. Biol. Chem.* **277**:33228–33234.
40. Yi, M., Y. Ma, J. Yates, and S. M. Lemon. 2007. Compensatory mutations in E1, p7, NS2, and NS3 enhance yields of cell culture-infectious intergenotypic chimeric hepatitis C virus. *J. Virol.* **81**:629–638.